Cooperative Binding Isotherms for Nearest Neighbor Interacting Ligands on Platonic Solids: A Simple Model for Viral Capture Nanotherapy

ARTICLE *in* THE JOURNAL OF PHYSICAL CHEMISTRY B · OCTOBER 2010

Impact Factor: 3.3 · DOI: 10.1021/jp1066378 · Source: PubMed

Cooperative Binding Isotherms for Nearest Neighbor Interacting Ligands on Platonic Solids: A Simple Model for Viral Capture Nanotherapy

Ronald A. Siegel*,†,‡ and Jayne L. Linstad‡

Departments of Pharmaceutics and Biomedical Engineering, and Minnesota Supercomputing Institute, University of Minnesota, Minneapolis, Minnesota 55455, United States

Received: July 16, 2010

The binding polynomial formalism is used to calculate binding isotherms for nearest neighbor interacting ligands on the platonic solids, i.e., tetrahedron, cube, octahedron, dodecahedron, and icosahedron. The activity of ligand (concentration multiplied by intrinsic binding constant of ligand to single sites) at half occupancy is precisely determined by the product of the coordination number or valence of the vertices and the free energy of interaction, regardless of other geometrical and topological features. More importantly, the sharpness of binding curves increases with interaction strength, with Hill exponents approaching the number of binding sites per solid particle, i.e., the number of vertices or the number of faces. Potential applications of the model to viral capture nanotherapy are suggested.

Introduction

The purpose of this article is to calculate binding isotherms of ligands to platonic solids, where it is assumed that the ligand has a native binding affinity to either the vertices or faces of the solid and that nearest neighbor interactions between bound ligands are present. The presence of such interactions can lead to high binding cooperativity and a sharply enhanced apparent binding affinity.

There are several potential applications. First, viruses consist of DNA or RNA packaged inside a protein/lipid capsid, which typically self-assemble into structures exhibiting icosahedral symmetry. Viral capture therapy has been proposed in which all, or at least a large fraction, of the viral surface is covered with ligand, neutralizing and preventing import or export of the virus between the cell and its environment.[1−4] High binding cooperativity might be exploited to reduce the required native binding affinity of individual ligands to the virus by orders of magnitude. Various structures such as liposomes, dendrimers, polymer micelles, and platelet-shaped nano-objects, possessing both the binding ligand for the viral surface and domains for self-association with neighboring objects, might provide effective encapsulation of virus.

A second potential application is in nanoscience and technology and in colloids. With recent advances in nanosynthesis, particles can be produced with excellent size and shape fidelity.[5−9] It is not unreasonable to expect that monodisperse platonic solid particles of colloidal dimension can be synthesized. Colloidal stability or controlled flocculation and assembly of these particles might be mediated by thin functionalized nanoplates, also amenable to design. Self-assembly of platelets on the core particles can be initiated by native binding to individual faces but potentiated or inhibited by interactions between the nanoplates.

Cooperative sharpening of binding isotherms due to nearest neighbor interactions is well studied in various limits. On one end, nearest neighbor interactions between oxygen-bound subunits of hemoglobin were postulated many years ago to account for the sigmoidal shape of the oxygenation isotherm.[10,11] On the other end, the Ising lattice gas model deals with adsorption onto infinite linear chains and planar lattices and binding to higher dimensional lattice structures.[12−14] In one dimension, predicted isotherms are smooth but become progressively sharper as nearest neighbor interactions increase. In two and higher dimensions, lattice gas isotherms exhibit bistability when interactions exceed a threshold, indicative of a first-order phase transition. In the present model, the lattices are finite, closed and two-dimensional. We expect, a priori, that binding isotherms will not be bistable, but their sharpness will increase with interaction strength.

The binding polynomial formalism has been shown to be a convenient means to translate binding mechanisms into theoretical isotherms. Here we review binding polynomial theory and specialize it to the platonic solids, representing these solids as regular platonic graphs.[15] The potential relation of this theory to antiviral therapy based on cooperative binding of nano-objects to viral surfaces is discussed.

Binding Polynomials and Regular Graphs

Schellman[16] demonstrated how the grand canonical partition function of statistical mechanics, which is used in lattice gas theory,[13] can be adapted to predict ligand binding to macromolecules in solution, using the binding polynomial formalism. More recent discussions of the binding polynomial and its applications are given by Stigter and Dill,[17] Poland,[18] and Di Cera et al.[19] We now present a graph theoretical approach to the binding polynomial, with attention to symmetry properties that emerge with regular graphs.

A graph is a set of V vertices with a set of E edges connecting pairs of vertices.[15] A graph is considered to be connected if a sequence of edges links each vertex to every other vertex. We shall only consider connected graphs here. A convenient way to represent the topology of vertices and edges is through a $V \times V$ adjacency matrix, $\mathbf{A}$. When vertices i and j are connected by an edge, $\mathbf{A}_{ij} = 1$; otherwise $\mathbf{A}_{ij} = 0$. When $\mathbf{A}_{ij} = 1$, two vertices are called "adjacent" or "nearest neighbors". The

* Corresponding author. E-mail: siege017@umn.edu. Phone: 1-612-624-6164.
† Departments of Pharmaceutics and Biomedical Engineering.
‡ Minnesota Supercomputing Institute.

10.1021/jp1066378
Published on Web 10/15/2010

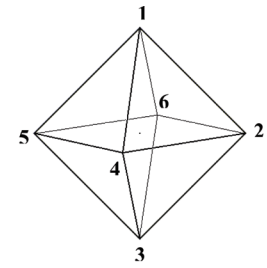

a)

$$\mathbf{A} = \begin{bmatrix} 0 & 1 & 0 & 1 & 1 & 1 \\ 1 & 0 & 1 & 1 & 0 & 1 \\ 0 & 1 & 0 & 1 & 1 & 1 \\ 1 & 1 & 1 & 0 & 1 & 0 \\ 1 & 0 & 1 & 1 & 0 & 1 \\ 1 & 1 & 1 & 0 & 1 & 0 \end{bmatrix}$$

b)

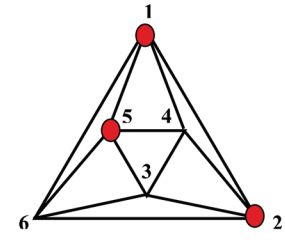

c)

$$\Gamma_0 = 1$$
$$\Gamma_1 = 6$$
$$\Gamma_2 = 3 + 12W$$
$$\Gamma_3 = 12W^2 + 8W^3$$
$$\Gamma_4 = 3W^4 + 12W^5 = W^4(3 + 12W)$$
$$\Gamma_5 = 6W^8$$
$$\Gamma_6 = W^{12}$$

d)

Figure 1. Relevant information for octahedron (O), $V = 6$, $E = 12$, $F = 8$. (a) Representation in 3D, showing labeling of vertices. (b) Adjacency matrix. For example, vertex 1 is connected to vertices 2, 4, 5, and 6 but not to itself or site 5. (c) Planar representation of O, with vertices 1, 2, and 5 liganded. Dashes indicated active edges joining adjacent liganded sites, which contribute weight W to the binding polynomial. In this example, $\mathbf{s}_\omega = (1,1,0,0,1,0)$, $\mathbf{s}_\varpi = (1,1,0,0,1,0)$, $v_\omega = 3$, $e_\omega = 2$, $e'_\omega = 8$, $e''_\omega = 2$. (d) Coefficients of the binding polynomial, $\Gamma_v(W)$, $v = 0, ..., V$. $\Gamma_0 = 1$ since there is only one way to have zero vertices liganded. $\Gamma_1 = 6$ since there are six ways to ligand single vertices. $\Gamma_2 = 3 + 12W$ since there are three ways of liganding pairs of vertices without sharing an edge (antipodes) and twelve ways to ligand pairs of vertices that share an edge. $\Gamma_3 = 12W^2 + 8W^3$ since there are twelve ways of liganding three vertices in a "row" and eight ways to ligand three vertices by forming triangles. Other Γ_i values are understood by similar reasoning. Note that the symmetry relation in eq 17 is obeyed.

number of nearest neighbors of a vertex, i, is called its valency or coordination number and is denoted by z_i. A graph is regular if all vertices have the same valency, z. By the handshake lemma, $zV = 2E$ for all regular graphs. As an illustrative example, a representation of the octahedral graph and its adjacency matrix are shown in Figures 1a,b.

In the present model, the vertices are assumed to be binding sites for ligands that are present in solution at a concentration denoted by c (M). Two parameters govern ligand binding. First, there is the native affinity, K (M^{-1}), of ligand for a single vertex. Second, there is the interaction weight, W (no units), between ligands bound to adjacent vertices. The cases $W = 1$, $W > 1$, and $W < 1$ correspond to neutral, favorable, and unfavorable interactions between adjacent bound ligands. We assume that K and W are constant and independent of context, i.e., specific binding pattern. Corresponding to K and W are the free energies $\Delta g_K = -k_BT \ln K$ and $\Delta g_w = -k_BT \ln W$, each containing enthalpic and entropic components, leading to the usual dependences on temperature, i.e., $K = e^{\Delta s_K} e^{-\Delta h_K/k_BT}$ and $W = e^{\Delta s_W} e^{-\Delta h_W/k_BT}$, where Δh and Δs are the associated enthalpy and entropy changes and k_BT is the Boltzmann temperature factor.

A particular ligand configuration, ω, on a graph is represented by the vertex occupancy vector, $\mathbf{s}_\omega = (s_1, ..., s_V)_\omega$ with $s_i = 1$ when the ith vertex is liganded and 0 otherwise. See Figure 1c for an example on the octahedron. The number of liganded vertices for the configuration is

$$v_\omega = (\sum_{i=1}^{V} s_i)_\omega \tag{1}$$

and the number of nearest neighbor interactions between bound ligands is

$$e_\omega = (\sum_{i=1}^{V-1} \sum_{j=i+1}^{V} \mathbf{A}_{i,j} s_i s_j)_\omega \tag{2}$$

We shall call e_ω the number of "active" edges in the configuration. In addition to the active edges, a configuration will contain e'_ω inactive edges leading from a liganded vertex to an unliganded vertex, and $e''_\omega = E - e_\omega - e'_\omega$ inactive edges connecting two unliganded vertices. Finally, for each ω there is a complementary configuration, ϖ, in which the ligation states of all vertices are reversed, i.e., $(\mathbf{s}_i)_\varpi = 1 - (\mathbf{s}_i)_\omega$. Clearly, $v_\varpi = V - v_\omega$, $e_\varpi = e''_\omega$, $e_\omega = e''_\varpi$, and $e'_\varpi = e'_\omega$.

The statistical weight of the ligand configuration ω is given in this model by

$$\Theta_\omega = W^{e_\omega}(Kc)^{v_\omega} \tag{3}$$

Summing the statistical weights corresponding to all possible ligand configurations on the graph, we obtain the partition function for ligand binding from free solution to the graph's vertices

$$\Gamma = \sum_\omega \Theta_\omega = \sum_\omega W^{e_\omega}(Kc)^{v_\omega} \tag{4}$$

By defining

$$\Gamma_v(W) = \sum_{v_\omega = v} W^{e_\omega} \tag{5}$$

the partition function is recast in the binding polynomial form

$$\Gamma = \sum_{v=0}^{V} \Gamma_v(W)(Kc)^v \tag{6}$$

Note that the Γ_v's are polynomials in W of varying degree which can be written as $\Gamma_v = \sum_{e=0}^{E} \gamma_{v,e} W^e$. Also note that $\Gamma_0 = \gamma_{0,0} = 1$ since there is one configuration with $v = 0$, and there are no active edges in this case. When there are no interactions among bound ligands ($W = 1$), $\Gamma = (1 + Kc)^V$, so

$$\Gamma_v(W = 1) = \frac{V!}{v!(V - v)!} \tag{7}$$

Figure 1d shows how the binding polynomial is developed on the octahedron.

The binding polynomial is of interest since it can be used to derive many observable properties of ligand binding. The ratio $\Gamma_v(W)(Kc)^v/\Gamma$ is the probability that v of the V vertices are liganded. The mean vertex occupancy, $\bar{v}$, or binding isotherm, is obtained using

$$\bar{\upsilon}(c) = \frac{\sum_{\upsilon=0}^{V} \upsilon\Gamma_\upsilon(W)(Kc)^\upsilon}{\sum_{\upsilon=0}^{V} \Gamma_\upsilon(W)(Kc)^\upsilon} = \frac{\partial \ln \Gamma}{\partial \ln c} \quad (8)$$

The second log derivative of the binding polynomial,

$$\sigma_\upsilon^2(c) = \frac{\partial^2 \ln \Gamma}{\partial(\ln c)^2} = \frac{\sum_{\upsilon=1}^{V} \upsilon^2\Gamma_\upsilon(W)(Kc)^\upsilon}{\sum_{\upsilon=0}^{V} \Gamma_\upsilon(W)(Kc)^\upsilon} - \bar{\upsilon}^2 \quad (9)$$

is the variance (mean squared dispersion) of vertex occupancy at a fixed ligand concentration. The quantity σ_υ^2 is also the sensitivity or "susceptibility" of vertex occupancy to small fractional changes in ligand concentration. Because of its dual interpretation, we call σ_υ^2 the fluctuation-susceptibility index. This index is of most importance where the isotherm is steep, as will be discussed below.

The development thus far applies to general graphs with active edges between liganded nearest neighbors. For regular graphs with valency z, $e'_\omega = z\upsilon_\omega - 2e_\omega$, since z edges emanate from each liganded vertex, and each active edge in ω connects two such vertices. Combining this observation with $e''_\omega = e_\varpi$ and $e''_\omega = E - e_\omega - e'_\omega$ yields $e_\varpi = e_\omega + (E - z\upsilon_\omega)$. From this identity, along with $\upsilon_\varpi = V - \upsilon_\omega$, we obtain

$$\Theta_\varpi = W^{e_\varpi}(Kc)^{\upsilon_\varpi} = W^{E-z\upsilon_\omega}W^{e_\omega}(Kc)^{V-\upsilon_\omega} \quad (10)$$

which combined with eqs 3−6 and $zV = 2E$ leads to an important relationship between binding polynomial coefficients

$$\Gamma_{V-\upsilon} = W^{E-z\upsilon}\Gamma_\upsilon = W^{z(V/2-\upsilon)}\Gamma_\upsilon \quad (11)$$

Define $c_{0.5}$ as the ligand concentration at which half of the vertices are occupied, i.e., $\bar{\upsilon}(c_{0.5}) = V/2$. Introducing eq 11 into eq 8, we find for regular graphs that

$$Kc_{0.5} = W^{-z/2} \quad (12)$$

Since $W = e^{-\Delta g_w/k_BT}$, $K = e^{-\Delta g_K/k_BT}$, it follows that

$$Kc_{0.5} = e^{-z\Delta g_w/2k_BT}, \ln Kc_{0.5} = -\frac{z\Delta g_w}{2k_BT}, \text{and } \ln c_{0.5} = -\frac{\Delta g_K}{k_BT} - \frac{z\Delta g_w}{2k_BT} \quad (13)$$

Thus, the concentration at half ligation depends only on the binding and interaction free energies and the valency, along with temperature. It does not, however, depend on other details such as number of vertices or graph structure beyond nearest neighbor topology.

Using eqs 8, 11, and 12, it can be also shown[19] that the binding isotherm on regular graphs exhibits odd log sigmoidal symmetry around the half-ligation point. That is, defining c' such that $Kc' = 1/(Kc)$, it follows that $\bar{\upsilon}(c') = V - \bar{\upsilon}(c)$, or equivalently

$$\bar{\upsilon}(Kc')/V - 0.5 = 0.5 - \bar{\upsilon}(Kc)/V \text{ when } \log_{10}(c/c_{0.5}) = -\log_{10}(c'/c_{0.5}) \quad (14)$$

Equivalent forms of eqs 12−14 are given in ref 13. These relations need not hold for nonregular graphs. For example, they fail for a graph with three vertices connected by only two edges but are correct for a triangle graph.

A customary form used to fit experimental isotherms is the Hill equation

$$\hat{\bar{\upsilon}} = \frac{V(c/c_{0.5})^n}{1 + (c/c_{0.5})^n} \quad (15)$$

where $c_{0.5}$ is the ligand concentration in solution corresponding to half occupancy of binding sites and n, the Hill exponent, is taken as a measure of cooperativity of binding. This phenomenological function possesses the odd log symmetry that was just identified for cooperative binding isotherms on regular graphs. In the following, we "fit" the Hill equation to isotherms calculated for platonic solids calculated from the binding polynomial.

For regular graphs and a specified value of W, eq 12 immediately prescribes $c_{0.5}$. There are many ways to select n. Two procedures will be highlighted here. In the "50% match" procedure, we set $n = n_{50}$ such that $\partial \ln \hat{\bar{\upsilon}}/(\partial \ln Kc)_{c_{0.5}} = \partial \ln \bar{\upsilon}/(\partial \ln Kc)_{c_{0.5}}$. From eqs 8, 9, 12, and 15

$$n_{50} = 4\sigma_\upsilon^2/V\Big|_{c_{0.5}} \quad (16)$$

In the "90/10" procedure,[20] we set $n = n_{90/10} = \log_{10}(81)/\log_{10}(c_{0.9}/c_{0.1})$, $c_{0.1}$, and $c_{0.9}$, signifying the concentrations corresponding to 10% and 90% ligation, respectively, as predicted by eq 8. Since $\log_{10}(c_{0.9}/c_{0.1}) = 2$ when binding events are independent ($W = 1$), it is apparent that $2/n_{90/10}$ estimates the number of decades of concentration over which the largest part of the transition occurs between the graphs's mostly unliganded and mostly liganded states, for a given value of V. In the limits $c \to 0$ and $c \to \infty$, $\bar{\upsilon} \to 0$, and V, respectively, while $\sigma_\upsilon^2 \to 0$ at both limits, indicating that the distributions become very narrow at low and high ligand concentrations.

We conclude this section by showing that for regular connected graphs $n_{50} \to V$ as $W \to \infty$. To see why, recall that $\Gamma_0 = 1$. From eqs 11 and 12, $\Gamma_V(Kc)^V = 1$ at $c = c_{0.5}$. All other terms, $\Gamma_\upsilon(Kc)^\upsilon$, $\upsilon = 1, ..., V - 1$, are of negative order in W at $c = c_{0.5}$, so $\Gamma \to 2$ as $W \to \infty$ in eq 6. Similarly, the term dominating the numerator in eq 14 converges to V^2 as $W \to \infty$. The limiting behavior of n_{50} follows upon combining these observations with $\bar{\upsilon} = V/2$ in eq 9 and substituting the result in eq 16.

Computational Results for the Platonic Solids

The five platonic solids are the tetrahedron (T), cube (C), octahedron (O), dodecahedron (D), and icosahedron (I). Faces of platonic solids are identical regular polygons. Each solid is characterized by its number of faces (F), vertices (V), and edges (E). Each face is bounded by g edges, and z edges meet at each vertex. The reader is reminded of these characteristics in Table

TABLE 1: Geometric Parameters of Platonic Solids (Polyhedra)[a]

	g	*z*	*F*	*V*	*E*
tetrahedron	3	3	4	4	6
cube	4	3	6	8	12
octahedron	3	4	8	6	12
dodecahedron	5	3	12	20	30
icosahedron	3	5	20	12	30

[a] g = # of edges bounding each face; z = coordination number of each vertex; F = # of faces; V = # of vertices; E = # of edges.

1. Application of graph theory concepts to these solids is apparent, and the handshake lemma is augmented to $gF = zV = 2E$.

Connecting centers of each face of a solid with centers of their nearest neighbors (those sharing edges with the original face), a dual solid is formed, and the dual of the dual is the original solid. T is its own dual; C is dual with O; and D is dual with T. In forming a dual, $F \rightarrow V$, $V \rightarrow F$, $g \rightarrow z$, $z \rightarrow g$, and $E \rightarrow E$, and results obtained for vertex binding in one solid carry over immediately to "face binding" to its dual.

Binding polynomials for ligands on the five platonic solids are displayed in Table 2. The binding polynomial for the tetrahedron is familiar from the work of Pauling[10] and Koshland et al.[11] It is of the lowest order and is simplest insofar as each power of Kc is multiplied by a single power of W. All subgraphs formed by connecting adjacent liganded vertices on a tetrahedron are, for a given number of liganded vertices, topologically equivalent. For the higher solids, there are a multitude of subgraph topologies involved for a given number of liganded vertices. These topologies may include multiple connected components including trees, cycles, and polycycles with dangling ends. The multiple topologies underly the form of the $\Gamma_v(W)$ polynomials. As a simple example, there are three ways to place ligands on two vertices of O such that they are not adjacent and twelve such placements with the two vertices adjacent, hence $\Gamma_2(W) = 3 + 12W$ (Figure 1d). The most complex binding polynomial, by far, is associated with the dodecahedron, with 20 vertices and only 3 edges emanating from each vertex, leading to a rich variety of subgraph topologies.

It is readily verified that eq 11 holds in all cases. From Table 2, it is seen that

$$\Gamma_v(W) = W^{r(v)}\Gamma_v^*(W) \tag{17}$$

where $r(v)$ is a nonnegative integer and $\Gamma_v^*(W)$ is a polynomial with a nonnegative integer constant term. As predicted by eq 11, $\Gamma_v^*(W) = \Gamma_{V-v}^*(W)$ and $r(V - v) = E - zv + r(v)$. The exponent $r(v)$ is the minimum number of active edges resulting from v liganded vertices. For each solid there is a $v^* < V/2$ such that $r(v) = 0$ and $r(V - v) = E - zv$ for $v \leq v^*$. For example, in the octahedral lattice, $\Gamma_2^*(W) = \Gamma_4^*(W)$ but $r(2) = 0$, while $r(4) = 4$. For $v \leq v^*$, vertices can be liganded such that no two of them are nearest neighbors; i.e., there are no active edges. Higher-order terms of $\Gamma_v^*(W)$ correspond to ligand configurations with active edges. For $v > v^*$, the liganded vertices are too dense on the polyhedron to permit a "loner", and at least one active edge must exist; so, $\gamma_{v,0} = 0$. There can also be loner unliganded vertices, and each of these contributes z inactive edges.

Binding isotherms are calculated from eq 8. For example, the isotherm for the tetrahedron is well-known[10,11]

$$\bar{v} = \frac{4(Kc) + 12W(Kc)^2 + 12W^3(Kc)^3 + 4W^6(Kc)^4}{1 + 4(Kc) + 6W(Kc)^2 + 4W^3(Kc)^3 + W^6(Kc)^4}$$

The next simplest isotherm is for the octahedron,

$$\bar{v} = [6(Kc) + (6 + 24W)(Kc)^2 + (36W^2 + 24W^3)(Kc)^3 + W^4(12 + 48W)(Kc)^4 + 30W^8(Kc)^5 + 6W^{12}(Kc)^6]/[1 + 6(Kc) + (3 + 12W)(Kc)^2 + (12W^2 + 8W^3)(Kc)^3 + W^4(3 + 12W)(Kc)^4 + 6W^8(Kc)^5 + W^{12}(Kc)^6]$$

Isotherms become very complex for the higher solids, and it is interesting to determine how well the simple Hill approximation, eq 15, reflects isotherm behavior.

Figure 2a displays isotherms for O, with interaction weights $W = 1$, 2, 10, and 0.1, corresponding, respectively, to independent binding, weak and strong positive cooperativity, and negative cooperativity. For $W = 1$, Langmuirian behavior is produced. For $W = 2$, 10, the isotherms are sharpened, and its midpoint is shifted to the left, indicating high cooperativity. Both Hill approximations are also shown for these cases. The curves differ somewhat for $W = 2$, reflecting the disparity in the calculated Hill coefficients, $n_{50} = 2.20$ and $n_{90/10} = 1.86$. For $W = 10$, the Hill curves are virtually indistinguishable from each other ($n_{50} = 5.72$, $n_{90/10} = 5.65$) and from the exact curve.

For the anticooperative case, $W = 0.1$, the binding curve for O is shifted to the right and exhibits some waviness, which is readily explained. The first pair of vertices to be liganded will most often be antipodal (e.g., **1** and **3** in Figure 1a). The next pair will also most likely be antipodal (e.g., **2** and **5**), but more "chemical work" is required to bind ligands to them due to repulsion from the already bound ligands. The last pair (**4** and **6**) will require even more chemical work. The Hill approximation, which cannot reproduce the wavy behavior, is meaningless and hence is not shown. The anticooperative case is of lesser interest here, so further analysis will not be pursued.

Figure 2b displays normalized isotherms ($\bar{v}/V$) with $W = 1$ and 10, for all of the platonic solids. These curves are identical for $W = 1$, reflecting independent Langmuirian binding to each vertex. For $W = 10$, all isotherms are shifted to the left, and sharpness increases with number of vertices (see below however). Values of $Kc_{0.5}$ are identical for T, C, and D but are progressively lower for O and I. All normalized isotherms exhibit odd log symmetry around the ($Kc_{0.5}$, 0.5) point, consistent with eq 14.

Figure 3a displays values of $Kc_{0.5}$ as a function of W in log−log form. These values were taken from the calculated isotherms. Solid lines corresponding to eq 12 provide an exact fit. While eq 12 was derived in the previous section, it is remains remarkable that $Kc_{0.5}$ exhibits identical dependence on W for T, C, and D, even though binding patterns and correlations differ among the solids.

Figure 3b is a plot of the Hill coefficients n_{50} and $n_{90/10}$ over several log orders of W. As expected, cooperativity increases with interaction strength. We find for all platonic solids that $n_{50} > n_{90/10}$ for $W > 1$, while the opposite holds for $W < 1$. (As noted before, the latter case is not of interest.) For $W > 1$, n_{50} and $n_{90/10}$ do not differ greatly, and they both converge to V at high values of W, indicating that when nearest neighbor interactions are very strong the whole solid acts as a unit in its binding behavior. This convergence property was proved for n_{50} in the previous section. Still focusing on $W > 1$ and comparing the 3-valent solids, the Hill coefficient increases in

TABLE 2: Binding Polynomials Γ for Platonic Solids

Tetrahedron
$1 + 4(Kc) + 6W(Kc)^2 + 4W^3(Kc)^3 + W^6(Kc)^4$
Cube
$1 + 8(Kc) + (16 + 12W)(Kc)^2 + (8 + 24W + 24W^2)(Kc)^3 + (2 + 30W^2 + 32W^3 + 6W^4)(Kc)^4 + W^3(8 + 24W + 24W^2)(Kc)^5 + W^6(16 + 12W)(Kc)^6 + 8W^9(Kc)^7 + W^{12}(Kc)^8$
Octahedron
$1 + 6(Kc) + (3 + 12W)(Kc)^2 + W^2(12 + 8W)(Kc)^3 + W^4(3 + 12W)(Kc)^4 + 6W^8(Kc)^5 + W^{12}(Kc)^6$
Dodecahedron
$1 + 20(Kc) + (160 + 30W)(Kc)^2 + (660 + 420W + 60W^2)(Kc)^3 + (1510 + 2220W + 975W^2 + 140W^3)(Kc)^4 + (1912 + 5640W + 5340W^2 + 2300W^3 + 300W^4 + 12W^5)(Kc)^5 + (1240 + 7230W + 12900W^2 + 11660W^3 + 4920W^4 + 750W^5 + 60W^6)(Kc)^6 + (320 + 4380W + 14580W^2 + 24060W^3 + 21900W^4 + 10200W^5 + 1840W^6 + 240W^7)(Kc)^7 + (5 + 930W + 7080W^2 + 21440W^3 + 35655W^4 + 36420W^5 + 19010W^6 + 4740W^7 + 660W^8 + 30W^9)(Kc)^8 + W^2(900 + 7240W + 22440W^2 + 42540W^3 + 49940W^4 + 32220W^5 + 10740W^6 + 1760W^7 + 180W^8)(Kc)^9 + W^3(240 + 4380W + 16332W^2 + 37520W^3 + 54660W^4 + 45360W^5 + 21120W^6 + 4464W^7 + 660W^8 + 20W^9)(Kc)^{10} + W^5(900 + 7240W + 22440W^2 + 42540W^3 + 49940W^4 + 32220W^5 + 10740W^6 + 1760W^7 + 180W^8)(Kc)^{11} + W^6(5 + 930W + 7080W^2 + 21440W^3 + 35655W^4 + 36420W^5 + 19010W^6 + 4740W^7 + 660W^8 + 30W^9)(Kc)^{12} + W^9(320 + 4380W + 14580W^2 + 24060W^3 + 21900W^4 + 10200W^5 + 1840W^6 + 240W^7)(Kc)^{13} + W^{12}(1240 + 7230W + 12900W^2 + 11660W^3 + 4920W^4 + 750W^5 + 60W^6)(Kc)^{14} + W^{15}(1912 + 5640W^1 + 5340W^2 + 2300W^3 + 300W^4 + 12W^5)(Kc)^{15} + W^{18}(1510 + 2220W + 975W^2 + 140W^3)(Kc)^{16} + W^{21}(660 + 420W + 60W^2)(Kc)^{17} + W^{24}(160 + 30W)(Kc)^{18} + 20W^{27}(Kc)^{19} + W^{30}(Kc)^{20}$
Icosahedron
$1 + 12(Kc) + (36 + 30W)(Kc)^2 + (20 + 120W + 60W^2 + 20W^3)(Kc)^3 + W(30 + 195W + 180W^2 + 60W^3 + 30W^4)(Kc)^4 + W^3(120 + 300W + 252W^2 + 60W^3 + 60W^4)(Kc)^5 + W^5(72 + 340W + 300W^2 + 120W^3 + 80W^4 + 12W^5)(Kc)^6 + W^8(120 + 300W + 252W^2 + 60W^3 + 60W^4)(Kc)^7 + W^{11}(30 + 195W + 180W^2 + 60W^3 + 30W^4)(Kc)^8 + W^{15}(20 + 120W + 60W^2 + 20W^3)(Kc)^9 + W^{20}(36 + 30W)(Kc)^{10} + 12W^{25}(Kc)^{11} + W^{30}(Kc)^{12}$

the order T→C→D. On the other hand, the Hill coefficients for O initially exceed but cross below those for C and I, while the curve for I crosses from above to below the curve for D. Evidently, at lower values of W the nearest neighbor connections dominate cooperativity, while at higher values of W correlations at larger topological distances become important, until the whole solid is correlated.

Discussion and Conclusions

As initially discussed, the platonic solids are finite objects, differing from infinite lattice gases of two or more dimensions in that there is no phase transition in vertex occupancy. However, when interactions between adjacent ligands are strong, the transition is sharp. For large values of W and near the point of half occupancy, there will occur a kind of "phase separation" between compact clusters of liganded vertices and regions of unliganded vertices, especially for the higher solids D and I. In this respect, the higher solids behave like infinite lattices.

The present model was developed with viral capture therapy in mind. Previously, multivalent ligands have been studied for antiviral therapies, with substantial increases in binding affinities due to the enforced proximity of ligands on the same chain and the reduced translational entropy penalty associated with binding, compared to that which would be incurred when independent ligands simultaneously bind.[1] For example, sialic acid residues have been attached to polyacrylamide chains, and the construct's binding to influenza blocks the virus's sialic acid binding sites and provides a polymeric "halo" around the virion, thus inhibiting viral attachment to cells.[2] In other work, the multiple sialic acids were attached to dendrimers and liposomes to provide multivalent attachment.[3] Multivalent approaches have since been considered for a variety of viruses.[2−4] Here we suggest that such approaches could be enhanced by further conjugating the polymers or liposomes with moieties that promote "lateral" interactions. For example, ligand-terminate peptide blocks have been designed to self-assemble on viral surfaces.[4]

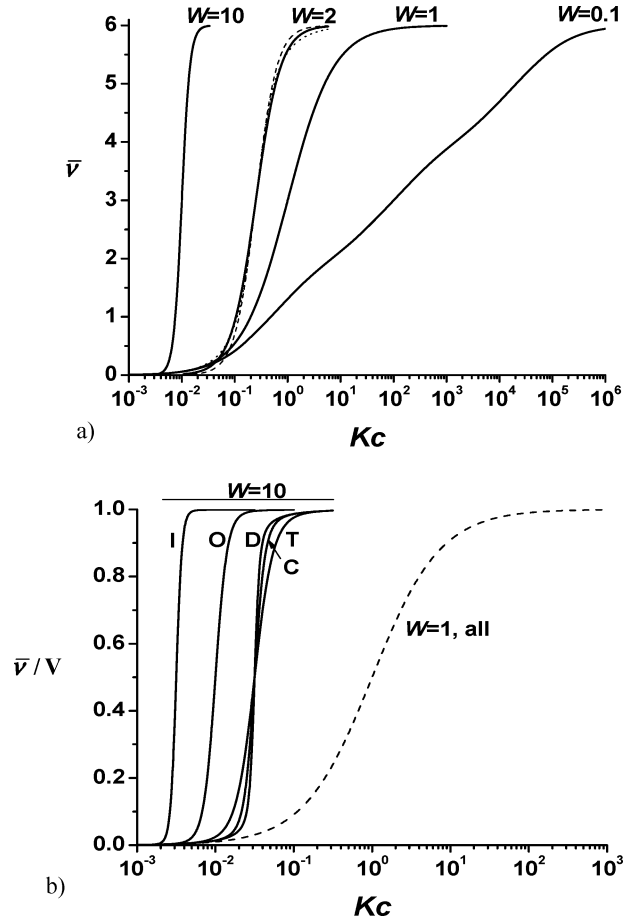

Figure 2. (a) Binding isotherms for octahedron, with neutral (W = 1), cooperative (W = 2, 10), and anticooperative (W = 0.1) interactions. Solid curves are exact isotherms, eq 10. Dashed and dotted lines for W = 2 are Hill equation fits, eq 15, with $n = n_{50}$ and $n = n_{50}$, respectively. (b) Binding isotherms, normalized to total number of vertices (V), for the platonic solids: T = tetrahedron, C = cube, O = octahedron, D = dodecahedron, I = icosahedron.

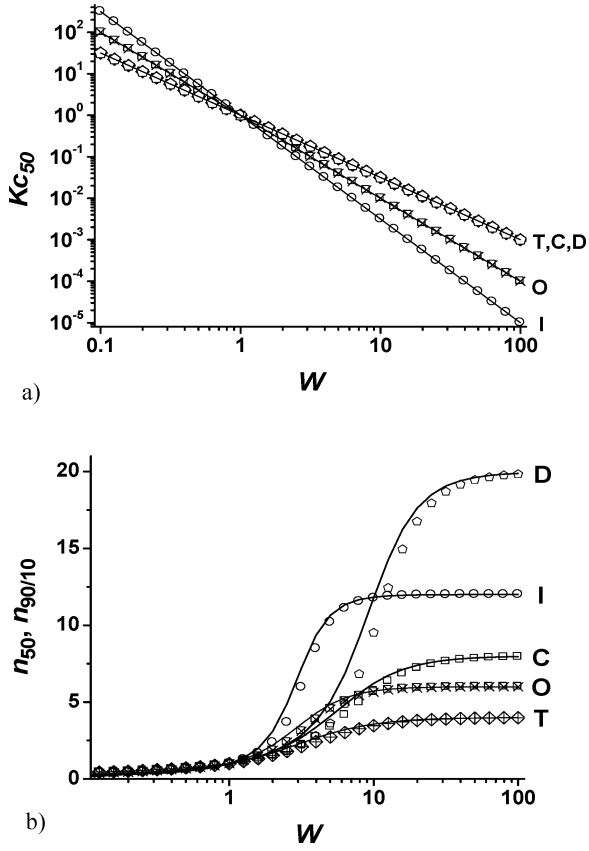

Figure 3. (a) Activities ($Kc_{0.5}$) at half ligand occupancy and (b) Hill coefficients (n_{50} and $n_{90/10}$) for the platonic solids, as a function of W: T = tetrahedron, C = cube, O = octahedron, D = dodecahedron, and I = icosahedron. Solid lines in (a) are predictions from eq 11, and symbols are points taken directly from calculated isotherms. Solid lines in (b) are n_{50}, and symbols are $n_{90/10}$.

The platonic solids, including the dodecahedron and icosahedron, are oversimplified models of real viruses. While viruses typically exhibit icosahedral symmetry in the large, capsids are often formed by assembly of capsomer "tiles" of different shapes. For example, vertices may consist of five pentagonal capsomers, with the hexagonal or otherwise shaped capsomers filling the icosahedral faces according to various geometric rules.[21−24] Design of self-assembling capture therapeutics would need to take these details into account.

Another biological object of interest is the endocytotic coated pit, which is formed by self-assembly of clathrin triskelion "monomers" into a variety of polyhedra, all with $z = 3$ but with a variety of pentagonal and hexagonal faces.[25−28] Coat proteins, COPI and COPII, associated with intracellular vesicular transport, also self-assemble into regular polyhedral cages. While COPI has a triskelion monomer with $z = 3$,[29] COPII has a different subunit structure that directs it to form regular polyhedra with $z = 4$.[30] All these assemblies, which also may be subject to cooperative pharmacologic modulation, are archimedian solids. Their vertices and edges form regular graphs, but their duals do not. An extension of the present work to archimedian solids and their duals may be of interest for future investigation.

Acknowledgment. This work was funded in part by a summer research fellowship to JLL from the Minnesota Supercomputer Institute. RAS thanks Prof. Ken A. Dill and Dr. Steve Pressé (University of California at San Francisco) for helpful discussions and computer resources provided during a sabbatical visit. This article is dedicated to the memory of Dr. Dirk Stigter.

References and Notes

(1) Mammen, M.; Choi, S.-L.; Whitesides, G. M. Polyvalent Interactions in Biological Systems: Implications for Design and Use of Multivalent Ligands and Inhibitors. *Angew. Chem., Int. Ed.* **1998**, *37*, 2754–2794.

(2) Sigal, G. B.; Mammen, M.; Dahman, G.; Whitesides, G. M. Polyacrylamides Bearing Pendant α-Sialoside Groups Strongly Inhibit Agglutination of Erythrocytes by Influenza Virus: The Strong Inhibition Reflects Enhanced Binding through Cooperative Polyvalent Interactions. *J. Am. Chem. Soc.* **1996**, *118*, 3789–3800.

(3) Choi, S.-K. *Synthetic Multivalent Molecules*; Wiley-Interscience: Hoboken, NJ, 2004.

(4) Gambaryan, A.; Boravleva, E. Y.; Matrosovich, T. Y.; Matrosovich, M. N.; Klenk, H.-D.; Moiseeva, E. V.; Tuzikov, A. B.; Chinarev, A. A.; Pazyna, G. V.; Bovin, N. V. Polymer-Bound 6′ Sialyl-N-Acetyllactosamine Protects Mice Infected by Influenza Virus. *Antiviral Res.* **2005**, *68*, 116–123.

(5) Manoharan, V. N.; Elsesser, M. T.; Pine, D. J. Dense Packing and Symmetry in Small Clusters of Microspheres. *Science* **2004**, *301*, 483–487.

(6) Gratton, S.; Pohlhaus, P.; Lee, J.; Guo, J.; Cho, M.; DeSimone, J. Nanofabricated Particles for Engineered Drug Therapies: A Preliminary Biodistribution Study of Print Nanoparticles. *J. Controlled Release* **2007**, *121*, 10–18.

(7) Champion, J.; Katare, Y.; Mitragotri, S. Making Polymeric Micro- and Nanoparticles of Complex Shapes. *Proc. Natl. Acad. Sci.* **2007**, *104*, 11901–11904.

(8) Acharya, G.; Shin, C. S.; McDermott, M.; Mishra, H.; Park, H.; Kwon, I. C.; Park, K. The Hydrogel Template Method for Fabrication of Homogeneous Nanoparticles. *J. Controlled Release* **2009**, *141*, 314–319.

(9) Xiong, Y.; Xia, Y. Shape-Controlled Synthesis of Metal Nanostructures: The Case of Palladium. *Adv. Mater.* **2007**, *19*, 3385–3391.

(10) Pauling, L. The Oxygen Equilibrium of Hemoglobin and Its Structural Interpretation. *Proc. Natl. Acad. Sci* **1935**, *21*, 186–191.

(11) Koshland, D. E. J.; Nemethy, G.; Fillmer, D. Comparison of Experimental Binding Data and Theoretical Models in Proteins Containing Subunits. *Biochemistry* **1966**, *5*, 365–368.

(12) Lee, T. D.; Yang, C. N. Statistical Theory of Equations of State and Phase Transitions. Ii. Lattice Gas and Ising Model. *Phys. Rev.* **1952**, *87*, 410–419.

(13) Hill, T. L. *Statistical Mechanics*; Dover: New York, 1956.

(14) Baxter, R. J. *Exactly Solvable Models in Statistical Mechanics*; Academic Press: London, 1982.

(15) Wilson, R. J. *Introduction to Graph Theory*; Academic Press: New York, 1972.

(16) Schellman, J. A. Macromolecular Binding. *Biopolymers* **1975**, *14*, 999–1018.

(17) Stigter, D.; Dill, K. A. Free Energy of Electrical Double Layers: Entropy of Adsorbed Ions and the Binding Polynomial. *J. Phys. Chem.* **1989**, *93*, 6737–6743.

(18) Poland, D. Ligand-Binding Distributions in Biopolymers. *J. Chem. Phys.* **2000**, *113*, 4774–4784.

(19) Di Cera, E.; Hopfner, K.-P.; Wyman, J. Symmetry Conditions for Binding Processes. *Proc. Natl. Acad. Sci.* **1992**, *89*, 2727–2731.

(20) Goldbeter, A.; Koshland, D. E. J. Sensitivity Amplification in Biochemical Systems. *Q. Rev. Biophys.* **1982**, *15*, 555–591.

(21) Caspar, D.; Klug, A. Physical Principles in the Construction of Regular Viruses. *Cold Spring Harbor Symp. Quant. Biol.* **1962**, *27*, 1–24.

(22) Wikoff, W. R.; Liljas, L.; Duda, R. L.; Tsuruta, H.; Hendrix, R. W.; Johnson, J. E. Topologically Linked Protein Rings in the Bacteriophage Hk97 Capsid. *Science* **2000**, *289*, 2129–2133.

(23) Zandi, R.; Reguera, D.; Bruinsma, R. F.; Gelbart, W. M.; Rudnick, J. Origin of Icosahedral Symmetry in Viruses. *Proc. Natl. Acad. Sci* **2004**, *101*, 15556–15560.

(24) Twarock, R. Mathematical Virology: A Novel Approach to the Structure and Assembly of Viruses. *Phil. Trans. R. Soc. London A* **2006**, *364*, 3357–3373.

(25) Van Workum, K.; Douglas, J. Symmetry, Equivalence, and Molecular Self-Assembly. *Phys. Rev. E* **2006**, *73*, 031502−1–031502−17.

(26) Kirchhausen, T. Clathrin. *Annu. Rev. Biochem.* **2000**, *69*, 699–727.

(27) Wilbur, J. D.; Hwang, P. K.; Brodsky, F. M. New Faces of the Familiar Clathrin Lattice. *Traffic* **2005**, *6*, 346–350.

(28) Nossal, R. Energetics of Clathrin Assembly. *Traffic* **2001**, *2*, 138–147.

(29) Lee, C.; Goldberg, J. Strcuture of Coatamer Cage Proteins and the Relationship among COPI, COPII, and Clathrin Vesicle Coats. *Cell* **2010**, *142*, 123–132.

(30) Stagg, S. M.; Gurkan, C.; Fowler, D. M.; LaPointe, P.; Foss, T. R.; Potter, C. S.; Carragher, B.; Balch, W. E. Structure of Sec13/31 COPII Coat Cage. *Nature* **2006**, *439*, 234–238.

JP1066378